Photon production in relativistic heavy ion collisions with equilibrium and non-equilibrium QGP*

FU Yong-Ping(傅永平)[1)] LI Yun-De(李云德)

Department of Physics, Yunnan University, Kunming 650091, China

Abstract We consider the production sources of prompt and thermal photons which include the contribution of gluons in relativistic heavy ion collisions. Considering in our calculation the shadowing and iso-spin effects of the nucleus we can properly estimate the prompt photon production. We develop a new thermal jet-photon conversion mechanism which plays a vital role in the low transverse momentum region. The effect of the non-equilibrium quark-gluon plasma enhances the contribution of thermal photons.

Key words relativistic heavy ion collisions, quark-gluon plasma, photons production

PACS 12.38.Mh, 25.75.Nq, 21.65.Qr

1 Introduction

Quark-gluon plasma (QGP) has become the most important issue in the study of relativistic heavy ion collisions [1–15]. It is difficult to probe the properties of the hot QGP during the short creating and cooling time [16–20]. Fortunately, the mean free path of the electromagnetic radiation is much larger than the size of the QGP, so a possible way is available to probe the photon information which is emitted from the plasma. Theoretical efforts aim to identify various sources of the electromagnetic radiation which includes prompt and thermal photons [21–24]. The background photons can be subtracted from the inclusive photon spectrum by using the statistical techniques of mixed-events in experiments [18]. Therefore, the background photons will not be discussed in this article.

We examine the contribution of gluon-photons and find that the production of gluon-photons is also an important source of prompt photons in the low $P_{\rm T}$ region. The EMC shadowing and the iso-spin effect of the nucleus are also considered in the calculation of the prompt photon production, because with such a consideration one can avoid overestimating the prompt photon production in nucleus-nucleus collisions [18, 21].

The jet-photon conversion turns into an important photon production source in the QGP [25–33]. Compared with the traditional thermal photon spectrum of the Compton and annihilation process, the contribution of thermal jet-photons which is produced by secondary Compton and annihilation processes plays a vital role in the low $P_{\rm T}$ region.

The reaction $q\bar{q} \leftrightarrow gg$ controls the increase and decrease of the quark number in the QGP [34]. The imbalance of the reaction induces a modification of the chemical potential in the hydrodynamic equation which will change the temperature function [16]. The added chemical potential in the non-equilibrium hydrodynamic equation increases the slope of the temperature function. The temperature function is used to compute the integral of the production rate of thermal photons, so the effect of the chemical non-equilibrium QGP enhances the thermal photon contribution.

2 Prompt photon production in relativistic heavy ion collisions

The prompt photons can be divided into three categories. They are direct photons, fragmentation photons and gluon-photons. Direct photons are produced by the Compton ($qg \to q\gamma$) and annihilation ($q\bar{q} \to$

Received 22 March 2009

* Supported by National Natural Science Foundation of China (10665003)

1) E-mail: fuyongping44@yahoo.com.cn

$g\gamma$ (QCD), $q\bar{q}\to\gamma\gamma$ (QED)) processes. Fragmentation photons are those produced by jet-photon fragmentation from final state partons. Gluon-photons are produced by the finite quark one-loop ($gg\to g\gamma$, $gg\to\gamma\gamma$) contributions.

Before the QGP formation time τ_i, the production of direct photons and gluon-photons which are emitted from hard collisions of high energy partons is described by the cross section ($A+B\to\gamma/\gamma\gamma+X$) as follows [25]

$$E\frac{d\sigma}{d^3p} = \frac{1}{\pi}\int dx_a G_{A/a}(x_a,Q^2)G_{B/b}(x_b,Q^2)\times \frac{x_a x_b}{x_a-x_1}\frac{d\hat{\sigma}}{d\hat{t}}(a+b\to c+d), \quad (1)$$

where the subprocesses of parton collisions $d\hat{\sigma}/d\hat{t}$ have been listed in previous studies [25, 31]. These subprocesses are given by the leading order (direct photons) and quark one-loop (gluon-photons) QCD calculations. To consider the higher order contributions, we take the K correction factor as $K\sim1.5$ [21]. The Mandelstam variables are $\hat{s}=x_a x_b s$, $\hat{u}=-x_b x_T s/2$ and $\hat{t}=-x_a x_T s/2$ when the rapidity y is zero, where $x_T=2P_T/\sqrt{s}$, $x_b=x_a x_2/(x_a-x_1)$. Here s is the square of the total energy of the nucleon-nucleon collisions and P_T is the transverse momentum of a photon. The integral range of the momentum fraction x_a is $[1, x_1/(1-x_2)]$, where $x_1=x_2=x_T/2$.

The contribution of the prompt gluon-photons is shown in Fig. 1. The strong coupling parameters of $gg\to g\gamma(\alpha\alpha_s^3)$ and $gg\to\gamma\gamma(\alpha^2\alpha_s^2)$ are relatively smaller than the coupling parameters of the direct photon processes ($\alpha\alpha_s$), but gluons are ample in the low P_T region, therefore the contribution of the gluon-photons can not be ignored in relativistic heavy ion collisions [21, 25]. The prompt gluon-photon spectrum is higher than the prompt direct production in the region of $P_T<1.5$ GeV (RHIC) and $P_T<7$ GeV (LHC). Especially, the prompt gluon-photon spectrum is higher than the prompt fragmentation photon (α_s^2) spectrum in the region of $P_T<2$ GeV (LHC). In Pb-Pb collisions at $\sqrt{s}$=5.5 TeV and P_T=1.0 GeV the contribution of prompt gluon-photons is almost 62% of the total photon spectrum. In the region of 1.1 GeV$< P_T <$2.0 GeV the contribution of prompt gluon-photons is almost 6.2%−0.3% of the total photon production at LHC. Therefore, the production of prompt gluon-photons is an important source of prompt photons.

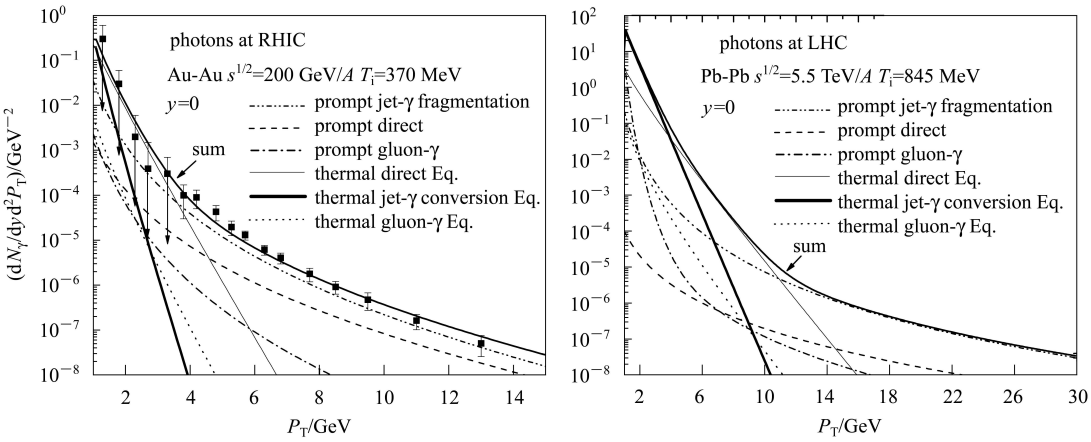

Fig. 1. The photon production sources in relativistic heavy ion collisions at RHIC (left) and LHC (right). Data at RHIC are from PHENIX [13].

We choose the parton distribution $G(x,Q^2)$ of the nucleus from M. Glück et al. [26] in the form $G(x,Q^2)=R(x,Q^2,A)[ZP(x,Q^2)+(A-Z)N(x,Q^2)]$, where $R(x,Q^2,A)$ is the EMC shadowing factor [27], Z is the proton number of the nucleus and A is the nucleon number. $P(x,Q^2)$ is the proton distribution, and $N(x,Q^2)$ is the neutron distribution. Since protons and neutrons have different distributions of up and down valence quarks ($u(x,Q^2)$ and $d(x,Q^2)$), the iso-spin effect of the nucleus can be represented by the sum of the proton and neutron distribution.

Previous studies treated the production rate of prompt photons by scaling the results for Proton-Proton collisions with the number of nucleon-nucleon collisions $\langle N_{coll}\rangle$ in the form [18, 21, 28] $dN_\gamma^{prompt}/(dyd^2P_T) = (Ed\sigma_{pp}/d^3p)(\langle N_{coll}\rangle/\sigma_{pp})$, where σ_{pp} is the mean cross section of P-P collisions, and $Ed\sigma_{pp}/d^3p$ is the cross section of P-P collisions which ignores the iso-spin and EMC shadowing effect of the nucleus. From Fig. 2 one can see that

the treatment without the shadowing and iso-spin effect will overestimate the prompt photon contribution in the high $P_{\rm T}$ region, the production rate of P-P collisions which ignore the iso-spin effect is higher than the result for N-N collisions in the higher region of $P_{\rm T}$ >5.5 GeV (RHIC) and $P_{\rm T}$ >8.5 GeV (LHC). We also discuss the shadowing effect at RHIC and LHC. If the shadowing factor is neglected, the prompt spectrum is also enhanced in the higher region of $P_{\rm T}$ >4.2 GeV (RHIC) and $P_{\rm T}$ >10.5 GeV (LHC). The effect of the shadowing and iso-spin weakly influences the prompt photon spectrum at RHIC, but the difference is more evident at LHC in the high $P_{\rm T}$ due to the shadowing factor and the sensitivity of the parton distributions to the collision energies.

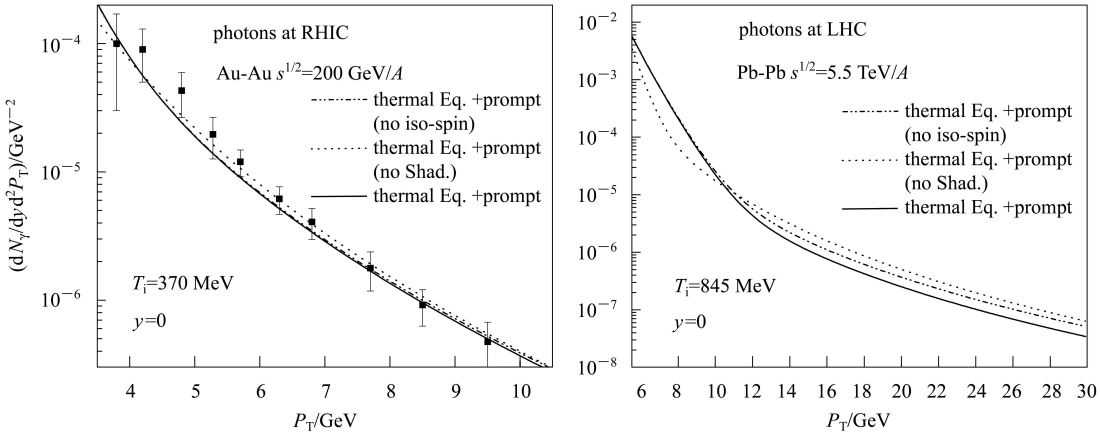

Fig. 2. The effect of the shadowing and iso-spin in Au-Au collisions at RHIC and Pb-Pb collisions at LHC. Data at RHIC are from PHENIX [13].

The cross section for the fragmentation photons is given as follows [31]

$$E\frac{\mathrm{d}\sigma}{\mathrm{d}^3p} = \int \mathrm{d}x_a \int \mathrm{d}x_b G_{A/a}(x_a,Q^2)G_{B/b}(x_b,Q^2)\times D_{\rm q}^{\gamma}(z_c,Q^2)\frac{1}{\pi z_c}\frac{\mathrm{d}\hat{\sigma}}{\mathrm{d}\hat{t}}(a+b\to c+d), \quad (2)$$

where $z_c = x_1/x_a + x_2/x_b$, and $\mathrm{d}\hat{\sigma}/\mathrm{d}\hat{t}$ represents the cross sections of Parton + Parton → Parton + Parton collisions. These subprocesses are $\mathrm{q_1q_2} \to \mathrm{q_1q_2}$, $\mathrm{q_1\bar{q}_2} \to \mathrm{q_1\bar{q}_2}$, $\mathrm{q_1q_1} \to \mathrm{q_1q_1}$, $\mathrm{q_1\bar{q}_1} \to \mathrm{q_2\bar{q}_2}$, $\mathrm{q_1\bar{q}_1} \to \mathrm{q_1\bar{q}_1}$, $\mathrm{q\bar{q}} \to \mathrm{gg}$, $\mathrm{gg} \to \mathrm{q\bar{q}}$, $\mathrm{qg} \to \mathrm{qg}$, $\mathrm{gg} \to \mathrm{gg}$, where the photon is emitted from the final state of the jet quark and described by introducing a photon fragmentation function $D_{\rm q}^{\gamma}(z_c,Q^2)$. The photon fragmentation function can be estimated from the Born approximation of the photon bremsstrahlung ($\mathrm{q} \to \gamma\mathrm{q}$) [25]. The integral range of momentum fractions are $x_a \in [1, x_1/(1-x_2)]$ and $x_b \in [1, x_a x_2/(x_a - x_1)]$. The fragmentation function of the photons is given by $D_{\rm q}^{\gamma}(z_c,Q^2) = (\alpha_{\rm s}/2\pi)\ln(Q^2/\Lambda^2) f_{\rm q}^{\alpha}(z_c)$, with $z_c f_{\rm q}^{\alpha}(z_c) = e_{\rm q}^2[1+(1-z_c)^2]$. A gluon can not couple with a photon, which means a gluon can not directly radiate a photon, so $D_{\mathrm{g}\to\gamma}^{\gamma}(z_c,Q^2) = 0$ [1, 25]. Here the strong running coupling constant is $\alpha_{\rm s} = 4\pi/[\beta_0 \ln(Q^2/\Lambda^2)]$, where the QCD scale parameter Λ=200 MeV and $\beta_0 = 11 - 2n_f/3$.

In Fig. 1, because the strong coupling parameter of the fragmentation processes ($\alpha_{\rm s}^2$) is higher than that of the direct processes ($\alpha\alpha_{\rm s}$), the fragmentation photons dominate the prompt photon spectrum in the high $P_{\rm T}$ region.

3 Thermal photon production in the equilibrium and non-equilibrium QGP

The energy-momentum conservation of the QGP fluid can be written in the form [1, 16, 21]

$$\partial_\mu T^{\mu\nu} = 0\,. \quad (3)$$

Considering the fact that the QGP is a chemical non-equilibrium fluid, the energy-momentum tensor can be written as $T^{\mu\nu} = (\epsilon + P')u^\mu u^\nu - g^{\mu\nu}P'$, where $P' = P - \mu n$, ϵ is the energy density, P is the pressure, μ is the chemical potential, n is the particle number, and u^μ is the four-velocity. The non-equilibrium process $\mathrm{q\bar{q}} \leftrightarrow \mathrm{gg}$ induces the imbalance of the quark number in the QGP. Then the chemical potential in the energy-momentum tensor can be written in the form $\mu n = \mu_{\rm q} n_{\rm q} + \mu_{\rm g} n_{\rm g}$, where $\mu_{\rm q}$ and $\mu_{\rm g}$ correspond to the chemical potentials of quarks and gluons. We assume that the states of the fermions are below the Fermi

surface, so the Fermi distribution is in the region of $0<\epsilon<\mu_{\rm q}$ and $\epsilon\gg T$. Finally the quark number and the energy density of quarks can be written in the form [17]

$$n_{\rm q}=\int_0^{\mu_{\rm q}}D_{\rm q}(\epsilon){\rm d}\epsilon=\int_0^{\mu_{\rm q}}\frac{4\pi\epsilon^2}{{\rm e}^{(\epsilon-\mu_{\rm q})/T}+1}{\rm d}\epsilon=\frac{4\pi}{3}\mu_{\rm q}^3, \quad (4)$$

and

$$\epsilon=\int_0^{\mu_{\rm q}}D_{\rm q}(\epsilon)\epsilon{\rm d}\epsilon=\frac{3}{4}n_{\rm q}\mu_{\rm q}. \quad (5)$$

Because the chemical potential of gluons is negative ($\mu_{\rm g}<0$), the gluon number and the energy density of gluons can be estimated as follows

$$n_{\rm g}=\int_0^{\infty}D_{\rm g}(\epsilon){\rm d}\epsilon=\int_0^{\infty}\frac{4\pi\epsilon^2}{{\rm e}^{(\epsilon-\mu_{\rm g})/T}-1}{\rm d}\epsilon=4\pi\mu_{\rm g}^2, \quad (6)$$

and

$$\epsilon=\int_0^{\infty}D_{\rm g}(\epsilon)\epsilon{\rm d}\epsilon=-n_{\rm g}\mu_{\rm g}, \quad (7)$$

where the Bose distribution is in the region of $\epsilon\geqslant|\mu_{\rm g}|$ and $\epsilon\gg T$. In the above integral the Bose distribution $f_B(\epsilon>|\mu_{\rm g}|)=0$ if the energy density $\epsilon\gg T$ [8, 17] and so the gluons have the distribution $f_B(\epsilon)=\delta(\epsilon-|\mu_{\rm g}|)$. The correlation between the pressure and energy density was given by previous studies in the form $P=\epsilon/3$ [1, 16]. Therefore, the hydrodynamic equation of the non-equilibrium fluid can be written in the form

$$\frac{\partial\epsilon}{\partial\tau}+\frac{\epsilon+P}{\tau}-\sum_{\rm i=q,g}\frac{\mu_{\rm i}n_{\rm i}}{\tau}=0. \quad (8)$$

The correlation between the time and temperature can be deduced from the hydrodynamic equation in the form

$$\left[\frac{T}{T_i}\right]^4=\frac{\tau_i}{\tau}. \quad (9)$$

Compared with the equilibrium result $[T/T_i]^3=\tau_i/\tau$ [16], the new correlation increases the slope of the temperature function. This temperature function is used to compute the time integral in the production rate of thermal photons, so the thermal photon spectrum is sensitive to the slope of the temperature function. In Fig. 3, one can see that the effect of the chemical non-equilibrium QGP enhances the spectrum of the total photons in the region of $P_{\rm T}<5$ GeV (RHIC) and $P_{\rm T}<14$ GeV (LHC).

We briefly recall the traditional thermal production rate of photons (Compton and annihilation). After the QGP formation time τ_i the emission rate of thermal direct photons can be written in the form [8]

$$\frac{{\rm d}N_\gamma^{\rm th-direct}}{{\rm d}y{\rm d}^2P_{\rm T}}=\int_{\tau_i}^{\tau_h}{\rm d}\tau\int_0^{V(\tau)}{\rm d}Vf_F(T)T^2M_{\rm q}(T), \quad (10)$$

where τ_h represents the critical time when the mixed phase transfers into the hadronic phase, $V(\tau)=\pi R_{\rm QGP}^2\tau$ describes the bulk of the system. We take the radius of the QGP as $R_{\rm QGP}\sim4-8$ fm (RHIC) and $R_{\rm QGP}\sim6-11$ fm (LHC) in the bulk integral [21]. The Compton integral factor is

$$M_{\rm q}^{\rm Com.}(T)=\frac{5}{9}\frac{4\alpha\alpha_{\rm s}}{96(2\pi)^2}\left[\ln\left(\frac{6P_{\rm T}}{\pi\alpha_{\rm s}T}\right)+C_{\rm Com}\right], \quad (11)$$

the one of the annihilation process is

$$M_{\rm q}^{\rm ann.}(T)=\frac{5}{9}\frac{4\alpha\alpha_{\rm s}}{18(2\pi)^2}\left[\ln\left(\frac{6P_{\rm T}}{\pi\alpha_{\rm s}T}\right)+C_{\rm ann}\right], \quad (12)$$

where the parameter $C_{\rm Com}=-0.42$ and $C_{\rm ann}=-1.92$ [8, 21]. Here α is the electromagnetic coupling constant and $f_F(T)$ is the Fermi-Dirac distribution.

Besides the thermal direct photons, one can not neglect other thermal sources in the QGP. Thermal photons also can be divided into three categories: thermal direct photons, thermal gluon-photons and thermal jet-photons. Thermal gluon-photons are produced from the processes of $gg\to g\gamma$ and $gg\to\gamma\gamma$. The production rate of thermal gluon-photons can be written in a similar form

$$\frac{{\rm d}N_\gamma^{\rm th-gluon}}{{\rm d}y{\rm d}^2P_{\rm T}}=\int_{\tau_i}^{\tau_h}{\rm d}\tau\int_0^{V(\tau)}{\rm d}Vf_B(T)T^2M_{\rm g}(T). \quad (13)$$

The integral factors of the thermal gluon-photons are

$$M_{\rm g}^{\rm gg\to\gamma\gamma}(T)=\frac{25}{81}\frac{4\alpha^2\alpha_{\rm s}^2}{192(2\pi)^3}\left[\ln\left(\frac{6P_{\rm T}}{\pi\alpha_{\rm s}T}\right)+C_{\rm g}\right] \quad (14)$$

and

$$M_{\rm g}^{\rm gg\to g\gamma}(T)=\frac{5}{12}\frac{4\alpha\alpha_{\rm s}^3}{192(2\pi)^3}\left[\ln\left(\frac{6P_{\rm T}}{\pi\alpha_{\rm s}T}\right)+C_{\rm g}\right], \quad (15)$$

where $f_B(T)$ is the Bose-Einstein distribution for gluons, and the parameter $C_{\rm g}$ is given by the following

$$C_{\rm g}=29.76-C_{\rm Euler}-\frac{6}{\pi^2}\sum_{n=1}^{\infty}\frac{\ln n}{n^2}=28.61, \quad (16)$$

where the parameter 29.76 comes from the mean cross section of $gg\to\gamma\gamma$ and $gg\to g\gamma$ given by

$$\sigma({\rm gg}\to\gamma\gamma)=\frac{25}{81}\frac{\alpha^2\alpha_{\rm s}^2}{16\hat{s}}\left[\ln\left(\frac{\hat{s}}{k_{\rm g}^2}\right)+29.76\right] \quad (17)$$

and

$$\sigma({\rm gg}\to{\rm g}\gamma)=\frac{5}{12}\frac{\alpha\alpha_{\rm s}^3}{16\hat{s}}\left[\ln\left(\frac{\hat{s}}{k_{\rm g}^2}\right)+29.76\right], \quad (18)$$

where $k_{\rm g}$ is an infrared cutoff [8].

In Fig. 1, one can see that the thermal direct spectrum is dominant in the region of $P_{\rm T}<3.7$ GeV (RHIC) and $P_{\rm T}<11$ GeV (LHC). The thermal gluon-photons make only a small contribution to the total thermal photons. We take the initial temperature T_i=370 MeV and the formation time τ_i=0.2 fm/c at RHIC and T_i=845 MeV τ_i=0.08 fm/c at LHC [21].

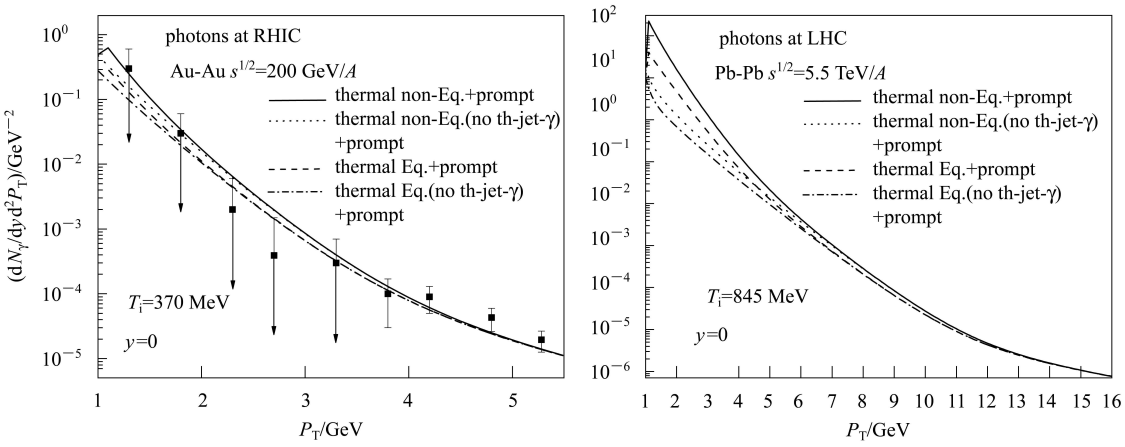

Fig. 3. The contribution of thermal jet-photons with the equilibrium and non-equilibrium condition at RHIC and LHC. Data at RHIC are from PHENIX [13].

In the parton model one can estimate the jet-photon fragmentation by introducing a photon fragmentation function into the hard scattering of partons. The photon fragmentation function is introduced from the Born approximation of the parton bremsstrahlung. Therefore, the QED bremsstrahlung $q \to \gamma q$ process plays an essential role in the jet-photon fragmentation. However, because of the jet quenching effect, the jet process in the hot quark-gluon medium is extremely suppressed and therefore the QED bremsstrahlung process is also suppressed in the quark-gluon medium.

A jet quark loses most of its energy in the process of the QCD bremsstrahlung $q \to gq$ due to the abundance of gluons in the low P_T, and the jet can no longer emit photons. However, a jet $q'/\bar{q}'$ crossing the hot gluon medium can convert into a photon by reacting with a quark or gluon via the Compton ($q'g \to \gamma q'$) and annihilation ($q'\bar{q}' \to \gamma g$) processes, where $q'/\bar{q}'$ represents the final state of the hard scattering $q'q' \to q'q'$ or $q'\bar{q}' \to q'\bar{q}'$ in the quark-gluon medium.

The expressions of the production rate of thermal jet-photons in the quark-gluon medium are

$$\frac{dN_\gamma^{\text{jet-Com.}}}{dyd^2P_T} = \xi(P_T)_{\text{jet-Com.}} \frac{dN_\gamma^{\text{th-Com.}}}{dyd^2P_T}, \tag{19}$$

and

$$\frac{dN_\gamma^{\text{jet-ann.}}}{dyd^2P_T} = \xi(P_T)_{\text{jet-ann.}} \frac{dN_\gamma^{\text{th-ann.}}}{dyd^2P_T}, \tag{20}$$

where the jet-conversion coefficients of the Compton and annihilation process are given by

$$\sqrt{\xi(P_T)_{\text{jet-ann.}}} = \xi(P_T)_{\text{jet-Com.}} = P_T^2 \frac{dN_{\text{jet}}^{qq\to qq}}{dyd^2P_T}. \tag{21}$$

The production rate of the jet quarks can be written in the form

$$\frac{dN_{\text{jet}}^{qq\to qq}}{dyd^2P_T} = \frac{1}{P_T^2}\int_{\tau_i}^{\tau_h} d\tau \int_0^{V(\tau)} dV E_q^2 f_F(T) \times T^2 M_{\text{jet}}(T), \tag{22}$$

where the integral factor is given by

$$M_{\text{jet}}(T) = \sum_{n=1}^{\infty} \frac{(-1)^{n+1}}{n^2} \frac{16\pi\alpha_s^2}{9(2\pi)^5} \times \left[\ln\left(\frac{6P_T}{\pi\alpha_s T}\right)^{1/2} - C_{qq}\right]. \tag{23}$$

Here the parameter C_{qq} comes from

$$C_{qq} = 0.773 + \ln\frac{1}{2} - \frac{C_{\text{Euler}}}{2} + \frac{\sum_{n=1}^{\infty} \frac{(-1)^{n+2}}{n^2}\ln n}{\sum_{n=1}^{\infty} \frac{(-1)^{n+1}}{n^2}} = -0.085, \tag{24}$$

where the parameter 0.773 is taken from the mean cross section $\sigma(qq \to qq)$ or $\sigma(q\bar{q} \to q\bar{q})$ in the form

$$\sigma(qq/q\bar{q} \to qq/q\bar{q}) = \frac{2}{9}\frac{\pi\alpha_s^2}{\hat{s}}\left[\frac{1}{2}\ln\frac{\hat{s}}{m_q^2} + 0.773\right]. \tag{25}$$

In the calculation of the mean cross section, we take the approximation as $\ln 0 \sim \ln(m_q/\sqrt{\hat{s}})$ due to the infrared cutoff of the integral divergence [8]. The differential cross section of the jet quark/antiquark scattering comes from Ref. [25].

Numerical results of the jet-photon conversion are shown in Figs. 1 and 3 at the RHIC and LHC energy. The jet-conversion coefficients depend sensitively on the system temperature and the thermal jet-photon spectrum can vary extremely with the different collision temperatures. At the RHIC (Fig. 1 left) temperature the contribution of thermal jet-photons enhances the total photon spectrum in the low region of

1 GeV< $P_{\rm T}$ <2.5 GeV, but the effect of the enhancement is not evident.

In the case of LHC (Fig. 1 right), the jet-photon conversion plays an important role in the thermal photon spectrum due to the rapidly rising jet-conversion coefficients with the higher system temperature. Thermal jet-photons are brighter than thermal direct photons in the interesting window 1 GeV< $P_{\rm T}$ <4 GeV at the temperature T_i=845 MeV. This window could be a good expectation for the LHC experimental data.

In Fig. 3, one can see the modification of thermal jet-photons in the total photon spectrum. At RHIC the contribution of thermal jet-photons enhances the total spectrum in the region of $P_{\rm T}$ <2.7 GeV (in the case of the non-equilibrium QGP), and $P_{\rm T}$ <2.2 GeV (in the case of the equilibrium QGP) (Fig. 3 left). The effect of the enhancement is more evident at LHC in the region of $P_{\rm T}$ <7.5 GeV (in the case of the non-equilibrium QGP), and $P_{\rm T}$ <6.8 GeV (in the case of the equilibrium QGP) (Fig. 3 right).

4 Conclusion

We have discussed various production sources of the electromagnetic radiation in relativistic heavy ion collisions. The contribution of gluon-photons is a vital modification of the prompt photon spectrum. Especially in Pb-Pb collisions at $\sqrt{s}$=5.5 TeV and $P_{\rm T}$=1.0 GeV the contribution of prompt gluon-photons is almost 62% of the total photon spectrum. In the region of 1.1 GeV< $P_{\rm T}$ <2.0 GeV the contribution of prompt gluon-photons is almost 6.2%–0.3% of the total photon production at LHC.

The treatment without the shadowing and iso-spin effect will overestimate the prompt photon production. Although the effect of the shadowing and iso-spin marginally influences the prompt photon spectrum at RHIC, these two effects will strongly impact on the correctness of the prompt photon spectrum at LHC.

Since the chemical potential of quarks and gluons increases the slope of the temperature function in the hydrodynamic equation, the effect of the non-equilibrium QGP enhances the thermal photon contribution.

A new jet-photon conversion mechanism for thermal photons has been developed. At RHIC, the contribution of thermal jet-photons enhances the total photon spectrum in the low region of 1 GeV< $P_{\rm T}$ <2.5 GeV. Especially at the LHC energy the jet-conversion coefficients rise rapidly and then thermal jet-photons become a novel shining source in the interesting window 1 GeV< $P_{\rm T}$ <4 GeV which could be a good expectation for the LHC experimental data.

References

1 Alam J, Srivastava D K et al. Phys. Rev. D, 1993, **48**: 1117
2 Fries R J, Müller B et al. Phys. Rev. Lett., 2003, **90**: 132301
3 Kapusta J, Lichard P et al. Nucl. Phys. A, 1992, **544**: 485
4 Ruuskanen P V. Nucl. Phys. A, 1992, **544**: 169
5 Hung C M, Shuryak E. Phys. Rev. C, 1998, **57**: 1891
6 Shuryak E and Xiong L. Phys. Rev. lett., 1993, **70**: 2241
7 Bass S A, Müller B et al. Phys. Rev. Lett., 2003, **90**: 082301
8 Kapusta J, Lichard P et al. Phys. Rev. D, 1991, **44**: 2774
9 Srivastava D K and Sinha B. Phys. Rev. Lett., 1994, **73**: 2421
10 Chatterjee R, Frodermann E S et al. Phys. Rev. Lett., 2006, **96**: 202302
11 Jeon S, Marian J J et al. Nucl. Phys. A, 2003, **715**: 795
12 Kolb P F, Sollfrank J et al. Phys. Rev. C, 2000, **62**: 054909
13 Adler S S et al. Phys. Rev. Lett., 2005, **94**: 232301; Adler S S et al. Phys. Rev. Lett., 2003, **91**: 072301
14 Albrecht R et al. Phys. Rev. Lett., 1996, **76**: 3506
15 Büsching H et al. Nucl. Phys. A, 2006, **774**: 103
16 Bjorken J D. Phys. Rev. D, 1983, **27**: 140
17 Huang K. Statistical Mechanics. New York: John Wiley and Sons, 1987; Landau L D and Lifshitz E M. Statistical Physics. Oxford: Pergamon Press, 1980.
18 Srivastava D K, Gale C et al. Phys. Rev. C, 2003, **67**: 034903
19 Turbide S, Rapp R et al. Phys. Rev. C, 2004, **69**: 014903
20 Kapusta J, Mclerran L D et al. Phys. Lett. B, 1992, **283**: 145
21 Turbide S, Gale C et al. Phys. Rev. C, 2005, **72**: 014906; Zhang Q H. hep-ph/0106242
22 Adams J et al. Phys. Rev. Lett., 2003, **91**: 172302
23 Adler C et al. Phys. Rev. Lett., 2003, **90**: 082302
24 Renk T. Phys. Rev. C, 2006, **74**: 034906
25 Berger E L, Braaten E et al. Nucl. Phys. B, 1984, **239**: 52
26 Glück M, Reya E et al. Z. Phys. C, 1992, **53**: 127
27 Qiu J. Nucl. Phys. B, 1987, **291**: 746
28 Jeon S, Marian J J et al. Phys. Lett. B, 2003, **562**: 45
29 Aurenche P, Fontannaz M et al. Phys. Rev. D, 2006, **73**: 094007
30 Chakrabarty S, Alam J et al. Phys. Rev. D, 1992, **46**: 3802
31 Combridge B L, Kripfganz J et al. Phys. Lett. B, 1977, **70**: 234
32 Kniehl B A, Kramer G et al. Nucl. Phys. B, 2000, **582**: 514
33 Cahn R N. Phys. Rev. D, 1973, **7**: 247
34 Gelis F, Niemi H et al. J. Phys. G: Nucl. Part. Phys., 2004, **30**: S1031